

# Observation of Magnon Damping Minimum Induced by Kondo Coupling in a van der Waals Ferromagnet $\text{Fe}_{3-x}\text{GeTe}_2$

Song Bao,<sup>1,\*</sup> Junsen Wang,<sup>2,3,\*</sup> Shin-ichiro Yano,<sup>4</sup> Yanyan Shangguan,<sup>1</sup> Zhentao Huang,<sup>1</sup>  
Junbo Liao,<sup>1</sup> Wei Wang,<sup>5</sup> Yuan Gao,<sup>6,2</sup> Bo Zhang,<sup>1</sup> Shufan Cheng,<sup>1</sup> Hao Xu,<sup>1</sup>  
Zhao-Yang Dong,<sup>7</sup> Shun-Li Yu,<sup>1,8</sup> Wei Li,<sup>2,†</sup> Jian-Xin Li,<sup>1,8,‡</sup> and Jinsheng Wen<sup>1,8,§</sup>

<sup>1</sup>*National Laboratory of Solid State Microstructures and Department of Physics, Nanjing University, Nanjing 210093, China*

<sup>2</sup>*CAS Key Laboratory of Theoretical Physics, Institute of Theoretical Physics, Chinese Academy of Sciences, Beijing 100190, China*

<sup>3</sup>*Center of Materials Science and Optoelectronics Engineering, College of Materials Science and Opto-electronic Technology,*

*University of Chinese Academy of Sciences, Beijing 100049, China*

<sup>4</sup>*National Synchrotron Radiation Research Center, Hsinchu 30077, Taiwan*

<sup>5</sup>*School of Science, Nanjing University of Posts and Telecommunications, Nanjing 210023, China*

<sup>6</sup>*School of Physics, Beihang University, Beijing 100191, China*

<sup>7</sup>*Department of Applied Physics, Nanjing University of Science and Technology, Nanjing 210094, China*

<sup>8</sup>*Collaborative Innovation Center of Advanced Microstructures, Nanjing University, Nanjing 210093, China*

In heavy-fermion systems with  $f$  electrons, there is an intricate interplay between Kondo screening and magnetic correlations, which can give rise to various exotic phases. Recently, similar interplay appears to also occur in  $d$ -electron systems, but the underlying mechanism remains elusive. Here, using inelastic neutron scattering, we investigate the temperature evolution of the low-energy spin waves in a metallic van der Waals ferromagnet  $\text{Fe}_{3-x}\text{GeTe}_2$  (Curie temperature  $T_C \sim 160$  K), where the Kondo-lattice behavior emerges in the ferromagnetic phase below a characteristic temperature  $T^* \sim 90$  K. We observe that the magnon damping constant diverges at both low and high temperatures, exhibiting a minimum coincidentally around  $T^*$ . Such an observation is analogous to the resistivity minimum as due to the single-impurity Kondo effect. This unusual behavior is described by a formula that combines logarithmic and power terms, representing the dominant contributions from Kondo screening and thermal fluctuations, respectively. Furthermore, we find that the magnon damping increases with momentum below  $T_C$ . These findings can be explained by considering spin-flip electron-magnon scattering, which serves as a magnonic analog of the Kondo-impurity scattering, and thus provides a measure of the Kondo coupling through magnons. Our results provide critical insights into how Kondo coupling manifests itself in a system with magnetic ordering and shed light on the coexistence of and interplay between magnetic order and Kondo effect in itinerant  $3d$ -electron systems.

The original Kondo effect, which takes the observed resistivity minimum in dilute magnetic alloys as one of its typical characteristics, describes the scattering of conduction electrons by magnetic impurities in dilute magnetic systems [1, 2]. This effect is classified as the single-impurity Kondo problem and is now well understood based on the density of states of conduction electrons and their coupling with the single-impurity spins [Fig. 1(a) and (d)] [1, 2]. The concept of Kondo physics has been extended to include the correlated electron systems, specifically those consisting of a dense periodic array of local moments interacting with the conduction electron sea through an antiferromagnetic Kondo interaction, referred to as a Kondo lattice [Fig. 1(b)-(e)] [2–5]. The Kondo-lattice model was initially proposed to describe the heavy-fermion state in  $f$ -electron systems, particularly in intermetallics containing Ce, Yb, or U elements [2–7]. In Kondo lattices, the Kondo effect can also induce an effective magnetic interaction between the localized spins, known as the Ruderman-Kittel-Kasuya-Yosida (RKKY) interaction, which can dominate the exchange coupling between neighboring localized spins.

The competition between the Kondo effect and couplings of localized spins underlies various intriguing phenomena in heavy-fermion compounds, including quantum criticality [8–11], strange-metal behavior [11, 12], and magnetism [13–16] and superconductivity [17, 18], which can be tuned by chemical doping, magnetic field or pressure [8–12]. In the strong Kondo coupling regime, the full hybridization between localized  $f$  electrons and the conduction electrons leads to the quenching of local moments and the expansion of the Fermi surface, resulting in the formation of a heavy Fermi-liquid state [Fig. 1(d) and (e)] [2–7, 19, 20]. Magnetic order can arise when the strength of the RKKY interaction exceeds the Kondo coupling [Fig. 1(e)]. Moreover, the coexistence of magnetic order with Kondo effect [13–16] or superconductivity [17, 18] can be observed, particularly in systems where the duality of  $f$  electrons emerges due to the mixed-valence situation and the multiorbital nature [13–18].

More recently, the unexpected heavy-fermion state has also been observed in certain  $d$ -electron transition metals, which reside in the intermediate regime between itineracy and localization of  $d$  electrons [21–31]. The understand-

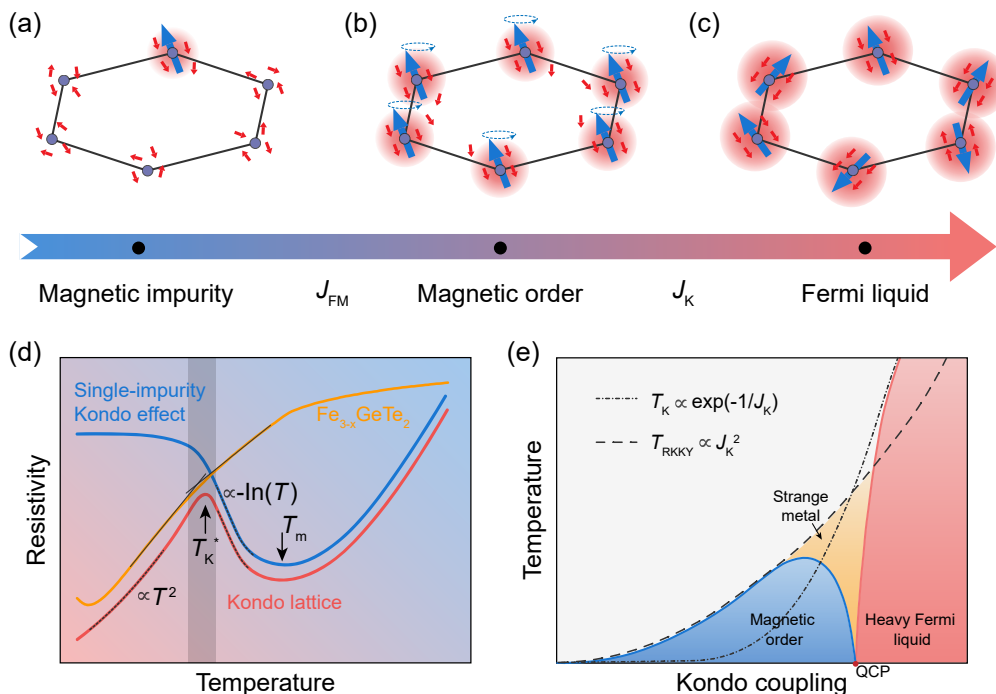


FIG. 1. (a)-(c) Schematic diagrams illustrating different scenarios of Kondo physics based on the concentration of local moments, the strength of ferromagnetic interaction  $J_{FM}$  and Kondo coupling  $J_K$ . (a) Kondo-impurity model, where local moments act as magnetic impurities. (b) Ferromagnetic Kondo-Heisenberg lattice model describing the case in  $Fe_{3-x}GeTe_2$ , where a dense periodic array of local moments aligns parallel to each other, giving rise to magnetic order through  $J_{FM}$ . Simultaneously, these local moments experience partial screening by the conduction electron sea, mediated by a weak  $J_K$ . (c) Heavy Fermi liquid, where local moments are quenched and a nonmagnetic heavy-fermion state forms with strong  $J_K$ . (d) Schematic illustration of the temperature-dependent resistivity for the three scenarios depicted in (a)-(c). For the two extreme cases in (a) and (c), upon cooling, resistivity encounters incoherent spin-flip scattering between localized spins and conduction electrons, resulting in a minimum and a  $-\ln(T)$  divergence below  $T_m$ . At lower temperatures, due to the formation of Kondo singlets, it becomes nearly temperature-independent in the Kondo-impurity model, while exhibiting Fermi-liquid behavior with a  $T^2$  scaling below the coherence temperature  $T_K^*$  in the Kondo-lattice model. For  $Fe_{3-x}GeTe_2$ , the resistivity exhibits a slope change at a characteristic temperature  $T^* \sim 90$  K, denoting an incoherent-coherent crossover represented by the shadow. (e) Canonical Doniach phase diagram of the Kondo lattice as a function of  $J_K$ , illustrating the magnetic ordering regime and heavy-fermion regime separated by a quantum critical point (QCP) [3, 4, 19]. The phase boundaries are determined by the energy scales of magnetic ordering temperature  $T_{RKKY}$  and Kondo temperature  $T_K$ .

ing of magnetism in the context of duality in these systems and the applicability of the Kondo-lattice model are currently active topics of research [21, 23, 25–31]. The van der Waals (vdW) metallic ferromagnet  $Fe_3GeTe_2$  is an example material. It has recently garnered attention due to the discovery of tunable room-temperature ferromagnetism down to the monolayer limit [32–35] and promising application potentials in magnetic vdW heterostructures [36, 37]. More importantly, previous studies reported the discovery of heavy-fermion state in this material, with intriguing electronic correlations, large effective electron mass renormalization, and the Kondo-lattice behavior [29–31, 38, 39].

Due to the coexistence of localized and itinerant  $3d$  electrons, it is not surprising that there is conflicting evidence regarding the microscopic origin of the magnetism in  $Fe_{3-x}GeTe_2$  [29–32, 40–43]. In our earlier work, we have reconciled the debate by showing that the ferro-

magnetism has a dual origin, with local moments and itinerant electrons contributing to the low-energy spin waves and columnlike continua, respectively [31]. Moreover, the Kondo coupling between local moments and itinerant electrons has also been reported [29–31]. It can be found that the resistivity curve of  $Fe_{3-x}GeTe_2$  reveals an incoherent-coherent crossover at a characteristic temperature  $T^*$ , as depicted in Fig. 1(d) (see also Refs. 29 and 31). Below  $T^*$ , the Kondo-lattice behavior emerges in the magnetic ordering phase, accompanied by the enhancement of Fermi surface volume and effective electron mass [29]. Notably, this resistivity behavior aligns with observations in other  $d$ -electron systems exhibiting a heavy-fermion state [22, 24, 25], but is distinct from either the Kondo-impurity model or the Kondo lattice in  $f$ -electron systems [Fig. 1(d)]. Our earlier work has also found that the interplay between local moments and itinerant electrons, manifesting as the Kondo screening

effect, is enhanced at low temperatures, resulting in a significantly heavier damping of spin waves at 4 K compared to 100 K [31]. Typically, magnons are well-defined and long-lived at low temperatures, and they gradually lose coherence upon warming due to the thermal fluctuations [44]. Given the presence of Kondo screening, how do spin excitations evolve with temperature?

In this Letter, we use inelastic neutron scattering (INS) to carefully study the temperature evolution of the low-energy spin waves in single crystals of Fe-deficient  $\text{Fe}_{3-x}\text{GeTe}_2$  with the Curie temperature  $T_C \sim 160$  K. We find that upon cooling from  $T_C$ , the damping of magnons will first decrease toward  $T^* \sim 90$  K and then increase rapidly, leaving a minimum at this intermediate temperature. We find it to be scaled with a linear combination of logarithmic and power terms, with these two terms corresponding to the Kondo coupling and thermal fluctuations, respectively. Furthermore, we find that the in-plane Kondo screening surpasses the out-of-plane screening, resulting in the softening of in-plane magnons at low temperatures. Our results provide smoking-gun evidence for the existence of Kondo effect in the metallic ferromagnet  $\text{Fe}_{3-x}\text{GeTe}_2$ , and demonstrate magnon damping as an effective measure for the Kondo coupling in systems where magnetic order and Kondo effect coexist.

The INS experiments on single crystals of  $\text{Fe}_{3-x}\text{GeTe}_2$  were performed on Sika located at the OPAL facility of ANSTO in Australia [45, 46]. Measurements were carried out using a fixed final-energy mode with  $E_f = 5.0$  meV, where both incident and final neutron energies were determined by pyrolytic graphite (002) crystals. An open-open-60'-60' collimation was used to strike a fine balance between neutron flux and experimental resolution. These settings gave an energy resolution of  $\sim 0.15$  meV at the elastic line. The  $\text{Fe}_{3-x}\text{GeTe}_2$  sample used in this measurement was the same as that used in Ref. 31, and was mounted in the  $(H, H, L)$  scattering plane. The wavevector  $\mathbf{Q}$  was expressed as  $(H, K, L)$  in reciprocal lattice unit (r.l.u.) of  $(a^*, b^*, c^*) = (4\pi/\sqrt{3}a, 4\pi/\sqrt{3}b, 2\pi/c)$  with refined lattice parameters  $a = b = 3.946$  Å and  $c = 16.357$  Å in a hexagonal structure.

Figure 2(a) and (b) show the energy scans at various temperatures for the off-centered in-plane and out-of-plane positions, respectively. Note that no sizable spin gap can be resolved at the Brillouin zone center, although there exists the magnetocrystalline anisotropy along the  $c$  axis [31]. From these raw scattering data, we can already find some unexpected features. For  $(-0.05, -0.05, 2)$  within the in-plane direction [Fig. 2(a)], no inelastic peak due to magnons can be observed at 4 K. Interestingly, the magnon peak appears at higher temperatures, but its center changes non-monotonically upon warming to  $T_C$ . For  $(0, 0, 1.7)$  within the out-of-plane direction [Fig. 2(b)], the peak center always shifts to lower energies upon warming. For both directions, the scat-

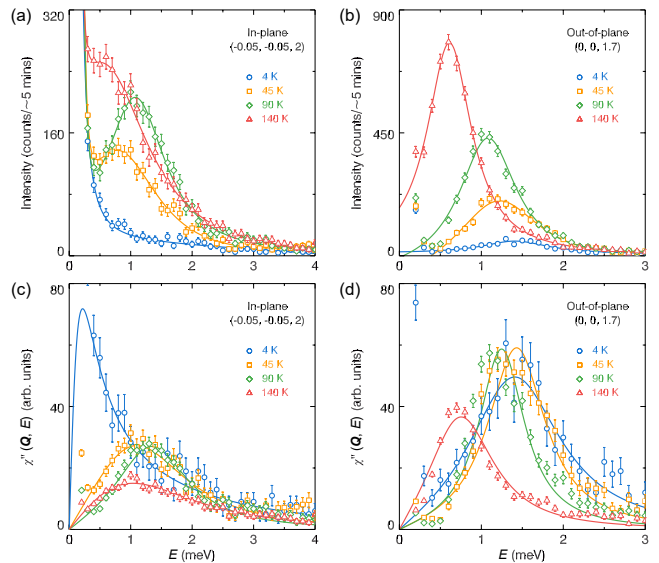


FIG. 2. (a) and (b) Temperature evolution of the energy scans off the Brillouin zone center at the in-plane position  $(-0.05, -0.05, 2)$  and out-of-plane position  $(0, 0, 1.7)$ , respectively. Different symbols represent different temperatures. Lines are guides to the eye with Lorentzian fittings. (c) and (d) Corresponding data of (a) and (b) after correction by the Bose population factor. Solid lines are fits with damped harmonic oscillator formulas described in the text. Throughout the paper, errors represent one standard deviation.

tering intensities increase with increasing temperature, which can be mainly ascribed to the Bose population factor that elevates the intensities at low energies and shifts the peak toward lower energies.

To eliminate the influence of the Bose statistics, we correct the raw data with the Bose population factor, and plot the corrected results in Fig. 2(c) and (d). As a result, the scattering intensities at different temperatures become comparable. We fit the corrected results with a damped harmonic oscillator (DHO) formula, which is applicable to damped spin waves [31, 47, 48]. The DHO formula has a form of  $\chi''(\mathbf{Q}, E) \propto \gamma E_0 E / [(E^2 - E_0^2)^2 + (\gamma E)^2]$ , where  $E_0$  is the magnon energy and  $\gamma$  is the damping constant (the inverse of  $\gamma$  is proportional to the lifetime of the damped magnons) [31, 47, 48]. Based on these DHO fittings shown in Fig. 2(c) and (d), we can extract the intrinsic magnon energy and the damping constant, which enables us to quantitatively characterize the temperature dependence of the magnons and their damping behaviors.

Figure 3 presents the extracted  $\gamma$  and  $E_0$  plotted as a function of temperature, showcasing the most intriguing results of this study. It is found that for both in-plane [Fig. 3(a)] and out-of-plane [Fig. 3(b)] directions,  $\gamma$  shows an upturn toward both 0 K and  $T_C$ , causing a minimum around  $T^* \sim 90$  K. Notably, this characteristic temperature is consistent with the incoherent-coherent

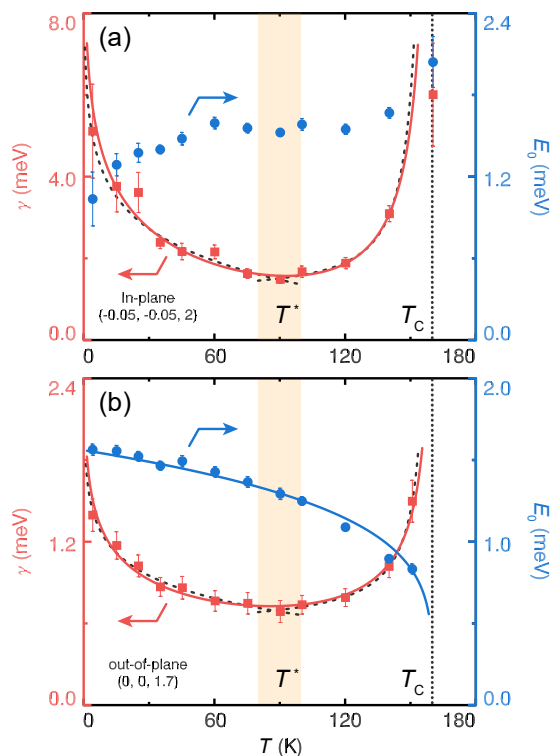


FIG. 3. The damping constant  $\gamma$  (red squares, left axis) and magnon energy  $E_0$  (blue circles, right axis) as a function of temperature, extracted from the DHO fittings to Bose-corrected data of the energy scans at  $(-0.05, -0.05, 2)$  [(a)] and  $(0, 0, 1.7)$  [(b)] at various temperatures. The dashed curves are guides to the eye fitted by either a single logarithmic or a single power function. The red solid curves are fits with the linear combination of these two terms. The blue solid curve in (b) is a fit with a simple power function.

crossover observed in the resistivity curve [Fig. 1(d)]. This phenomenon is reminiscent of the resistivity minimum caused by the Kondo effect in the original single-impurity Kondo model [Fig. 1(d)] [1–4], where thermodynamic and transport properties depend logarithmically on temperature as  $-\ln(T)$  [1–4]. Inspired by this, in Fig. 3, we use a similar logarithmic term to describe the divergent behavior toward 0 K. In the meantime, a power term normally describing the spin-wave damping in the hydrodynamic regime is also required to explain the divergence toward  $T_C$  [49, 50]. Actually, these two effects should exist simultaneously over the entire temperature range below  $T_C$ . Therefore, the general formula should consist of the linear combination of the two terms, which reads as,

$$\gamma(T) = A \ln(T^*/T) + B(1 - T/T_C)^{-\nu}. \quad (1)$$

To fit the data, we fix  $T^* = 90$  K and  $T_C = 160$  K, and allow  $A, B, \nu$  to be free parameters. The fitting results well reproduce the unusual non-monotonic temperature evolution of  $\gamma$  for both in-plane [Fig. 3(a)] and out-of-

plane [Fig. 3(b)] directions. Specifically, we obtain  $A_{\text{in}} = 1.556 \pm 0.254$ ,  $B_{\text{in}} = 0.888 \pm 0.129$ , and  $\nu_{\text{in}} = 0.692 \pm 0.108$  for the in-plane direction, and  $A_{\text{out}} = 0.316 \pm 0.019$ ,  $B_{\text{out}} = 0.530 \pm 0.022$ , and  $\nu_{\text{out}} = 0.382 \pm 0.027$  for the out-of-plane direction. The distinct parameter values for the in-plane and out-of-plane directions indicate the presence of magnetic anisotropy, which originates from the quasi-two-dimensional structure of  $\text{Fe}_{3-x}\text{GeTe}_2$ , consistent with our earlier magnetometry and neutron spectroscopy data on this material [31].

Other than the universal scaling of damping constant  $\gamma$ , the corresponding magnon energy  $E_0$  shown in Fig. 3 exhibits distinct behaviors for the in- and out-of-plane directions. With increasing temperature, it is found that the out-of-plane  $E_0$  softens through a power law while approaching  $T_C$  [Fig. 3(b)], a behavior similar to the temperature evolution of the magnetization in  $\text{Fe}_{3-x}\text{GeTe}_2$  [40, 51]. On the other hand, the in-plane  $E_0$  keeps almost constant across  $T^*$  and slightly softens upon cooling to lower temperatures [Fig. 3(a)]. We attribute these two distinct behaviors of  $E_0$  for the two directions to the different degrees of Kondo screenings. Note that the magnitude of  $\gamma$  for the in-plane direction is much larger than that for the out-of-plane direction, indicating a stronger screening effect for the in-plane direction. This can also be revealed from the ratio of the coefficients  $A_{\text{in(out)}}/B_{\text{in(out)}}$ , which roughly weighs the contribution to the magnon damping from the Kondo effect over the thermal broadening. It is 1.75 for the in-plane direction, about three times larger than that for the out-of-plane direction. When the Kondo screening is more significant for the in-plane direction, it can remarkably reduce the intralayer exchange coupling between local moments, resulting in a decrease in the in-plane  $E_0$  at low temperatures, as shown in Fig. 3(a). In some heavy-fermion compounds with  $f$  electrons, the phonon softening at low temperatures has been observed, which was attributed to the screening of atomic force [52, 53]. Intriguingly, phonon softening deviating from the anharmonic model has also been reported in  $\text{Fe}_{3-x}\text{GeTe}_2$  by the Raman measurements [54]. These findings indicate a complex correlation between electrons, lattice and magnetism in  $\text{Fe}_{3-x}\text{GeTe}_2$ .

To examine the momentum dependence of the damping, we plot the results of the low-energy spin-wave excitations and their damping constant as a function of momentum in Fig. 4. Let us take the excitations at 90 K as an example, where the spin waves are most coherent with the least damping (Fig. 3). The energy scans along [110] and [001] directions are plotted in Fig. 4(a) and (b), respectively. As  $Q$  increases, we observe a gradual shift in the peak center to higher energy, accompanied by a broadening of the linewidth and a weakening of the scattering intensities, indicating the nature of damped spin waves. We perform DHO fittings to these scans at various  $Q$ s to extract and plot the momentum dependence

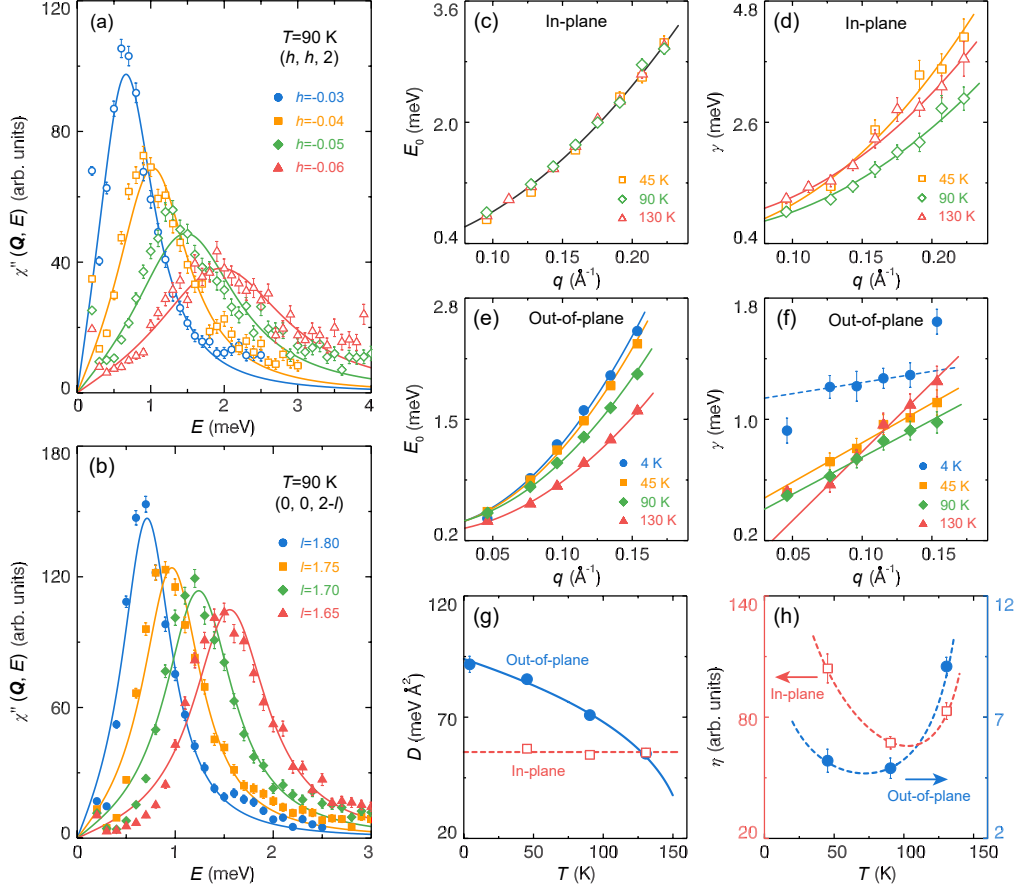


FIG. 4. (a) and (b) Corrected data of energy scans at different  $\mathbf{Q}$ s at 90 K along the in-plane direction  $(h, h, 2)$  and out-of-plane direction  $(0, 0, 2-l)$ , respectively. Solid lines are fits with DHO formulas. Extracted  $E_0$  (c) and  $\gamma$  (d) for the in-plane direction as a function of the off-centered wave vector  $q$  at 90 K and other temperatures. (e) and (f) Same as in (c) and (d) but for the out-of-plane direction. Lines in (c) and (e) are fits with quadratic functions. Lines in (d) and (f) are obtained with quasi-quadratic and linear fittings, respectively. In-plane and out-of-plane spin-wave stiffness (g) and damping coefficient (h) as a function of temperature. The solid curve in (g) is a fit with a simple power function and the dashed line is a guide to the eye. Dashed curves in (h) are guides to the eye with the form of Eq. 1.

of  $E_0$  [Fig. 4(c) and (e)] and  $\gamma$  [Fig. 4(d) and (f)] for the two directions. To fit these low-energy ferromagnetic spin waves at small  $\mathbf{Q}$ s, we use the quadratic dispersion relation of  $E_0 = \Delta + DQ^2$ , where  $\Delta$  is the spin gap and  $D$  is the spin-wave stiffness. The fittings give  $D$  of  $54.5 \pm 0.8 \text{ meV \AA}^2$  for the [110] direction [Fig. 4(c)] and  $70.9 \pm 1.1 \text{ meV \AA}^2$  for the [001] direction [Fig. 4(e)] at 90 K. Concerning  $\gamma$ , it appears to increase with  $\mathbf{Q}$  for both directions at the first glance. However, the detailed relationships with the reduced wavevector  $q$  differ, as they follow quasi-quadratic ( $\sim q^{2.2}$ ) [Fig. 4(d)] and linear dependencies [Fig. 4(f)] for the in-plane and out-of-plane directions, respectively.

The low-energy spin waves at other temperatures like 4, 45 and 130 K are also measured. With increasing temperature, we find that the spin-wave dispersion remains nearly unchanged for the in-plane direction but softens considerably for the out-of-plane direction [Fig. 4(c) and

(e)]. Note that since the in-plane spin waves are heavily damped at 4 K, it is challenging to extract a reasonable dispersion. It is found that the original  $q$ -dependences of  $\gamma$  for the two directions at 90 K remain applicable at other temperatures, *i.e.*,  $\gamma_{\text{in}} \sim \eta q^{2.2}$  and  $\gamma_{\text{out}} \sim \eta q$ . However, the magnitude and coefficient  $\eta$  of the damping vary due to the temperature dependence of the Kondo screening effect [Fig. 4(d) and (f)]. To better illustrate the temperature evolution of the spin waves, we plot the extracted spin-wave stiffness  $D$  and damping coefficient  $\eta$  as a function of temperature in Fig. 4(g) and (h), respectively. The out-of-plane  $D$  follows a typical power-law relationship with temperature, while the in-plane one remains nearly constant. For  $\eta$ , it follows a non-monotonic dependence and can also be traced by Eq. 1 for both directions. These findings further extend the results shown in Fig. 3 by investigating the magnetic excitations at different momenta, thereby uncovering a universal law governing the Kondo physics in  $\text{Fe}_{3-x}\text{GeTe}_2$ .



To the best of our knowledge, this is the first observation of a minimum in the magnon damping constant in heavy-fermion or Kondo-lattice systems. It is noteworthy that the minimum in magnon damping curve (Fig. 3) is closely related with the slope change in resistivity curve of  $\text{Fe}_{3-x}\text{GeTe}_2$  [Fig. 1(d)]. Unlike the full screening of local moments in the coherent Kondo lattice of some  $f$ -electron systems [Fig. 1(c)], we consider  $\text{Fe}_{3-x}\text{GeTe}_2$  demonstrates partial screening of local moments [Fig. 1(b)]. In this scenario, magnetic order by local moments is mediated by conduction electrons [32, 55], giving rise to the Kondo effect [29–31]. Below  $T^*$ , the localized electronic state hybridizes with the itinerant electronic state, enlarging the Fermi surface volume and effective electron mass [29]. Consequently, from the perspective of conduction electrons, the slope of resistivity changes, manifesting heavy-fermion behavior. Simultaneously, from the perspective of spin waves, these processes provide additional decay channels for the magnons, resulting in a significant damping of magnons below  $T^*$ .

In  $\text{Fe}_{3-x}\text{GeTe}_2$ , considering that direct exchange interactions and Kondo coupling dominate, a Ferromagnetic Kondo-Heisenberg lattice model [Fig. 1(b)] should be appropriate to understand our results. By treating conduction electrons as scatterers for the propagating magnons, we consider the second-order perturbation processes involving spin-flip scattering between conduction electrons and magnons to be crucial. In such processes, a magnon decays into a fermionic particle-hole pair and later reunites into a magnon. In this context, the magnon-electron interaction vertex is renormalized with a logarithmic temperature dependence, introducing a logarithmic scaling of the magnon damping rate at low temperatures, reminiscent of the single-impurity Kondo problem [1, 2]. By including the contribution to magnon self-energy due to magnon-magnon interactions, which diverges as a power law at relative high temperatures, the observed damping minimum can be reproduced in principle. Furthermore, since the kinetically allowed phase space for spin-flip scattering increases with increasing magnon momentum, the magnon damping becomes heavier with increasing momentum, in agreement with the experimental observation (Fig. 4). In our separate work [56], we have successfully reproduced the magnon damping minimum for a one-dimensional ferromagnetic Kondo-Heisenberg chain using tensor renormalization group methods. However, extending such protocols to higher-dimensional systems and obtaining analytical solutions for the magnon damping minimum remain challenging, which warrants further study.

In conclusion, our INS study of the temperature evolution of low-energy magnons in  $\text{Fe}_{3-x}\text{GeTe}_2$  reveals two main characteristics of magnon damping: a non-monotonic temperature dependence with logarithmic scaling below  $T^*$ , and an increase in damping with

momentum. Additionally, we find that the in-plane magnons undergo softening at low temperatures due to the more significant in-plane Kondo coupling. These findings provide important insights into the role of Kondo coupling in  $\text{Fe}_{3-x}\text{GeTe}_2$  from the perspective of magnons. They are consistent with other experimental observations in  $\text{Fe}_{3-x}\text{GeTe}_2$ , such as Fano resonance features in scanning tunneling microscopy measurements [29, 30], the heavy-fermion state inferred from angle-resolved photoemission spectroscopy measurements [29, 41] and the Sommerfeld coefficient [38], as well as the incoherent-coherent crossover in transport and magnetic measurements [29], which reflect the Kondo physics from the perspective of conduction electrons. Our work highlights magnon damping as an effective probe on the Kondo coupling in systems where magnetic order and Kondo effect coexist.

The work was supported by National Key Projects for Research and Development of China with Grant No. 2021YFA1400400, National Natural Science Foundation of China with Grant Nos. 12225407, 12074174, 12074175, 11904170, 11974036, 12222412, 12047503 and 12004191, Natural Science Foundation of Jiangsu province with Grant Nos. BK20190436 and BK20200738, Natural Science Foundation of the Higher Education Institutions of Jiangsu Province with Grant No. 23KJB140012, China Postdoctoral Science Foundation with Grant Nos. 2022M711569 and 2022T150315, Jiangsu Funding Program for Excellent Postdoctoral Talent No. 20220ZB5, and Fundamental Research Funds for the Central Universities. We acknowledge the neutron beam time from ANSTO with Proposal Nos. P9631 and P13772.

---

\* These authors contributed equally to the work.

† w.li@itp.ac.cn

‡ jxli@nju.edu.cn

§ jwen@nju.edu.cn

- [1] Jun Kondo, “Resistance Minimum in Dilute Magnetic Alloys,” *Prog. Theor. Phys.* **32**, 37–49 (1964).
- [2] Alexander Cyril Hewson, *The Kondo problem to heavy fermions* (Cambridge University Press, Cambridge, England, 1993).
- [3] Piers Coleman, *Introduction to many-body physics* (Cambridge University Press, Cambridge, England, 2015).
- [4] Eva Pavarini, Piers Coleman, and Erik Koch, *Many-body physics: from Kondo to Hubbard* (Theoretische Nanoelektronik, Jülich, Germany, 2015).
- [5] G. R. Stewart, “Heavy-fermion systems,” *Rev. Mod. Phys.* **56**, 755–787 (1984).
- [6] Stefan Kirchner, Silke Paschen, Qiuyun Chen, Steffen Wirth, Donglai Feng, Joe D. Thompson, and Qimiao Si, “Colloquium: Heavy-electron quantum criticality and single-particle spectroscopy,” *Rev. Mod. Phys.* **92**, 011002 (2020).
- [7] Hilbert v. Löhneysen, Achim Rosch, Matthias Vojta,

- and Peter Wölfle, “Fermi-liquid instabilities at magnetic quantum phase transitions,” *Rev. Mod. Phys.* **79**, 1015–1075 (2007).
- [8] A. Schröder, G. Aeppli, R. Coldea, M. Adams, O. Stockert, H.v. Löhneysen, E. Bucher, R. Ramazashvili, and P. Coleman, “Onset of antiferromagnetism in heavy-fermion metals,” *Nature* **407**, 351–355 (2000).
- [9] P. Gegenwart, J. Custers, C. Geibel, K. Neumaier, T. Tayama, K. Tenya, O. Trovarelli, and F. Steglich, “Magnetic-Field Induced Quantum Critical Point in  $\text{YbRh}_2\text{Si}_2$ ,” *Phys. Rev. Lett.* **89**, 056402 (2002).
- [10] J. Custers, P. Gegenwart, H. Wilhelm, K. Neumaier, Y. Tokiwa, O. Trovarelli, C. Geibel, F. Steglich, C. Pépin, and P. Coleman, “The break-up of heavy electrons at a quantum critical point,” *Nature* **424**, 524–527 (2003).
- [11] Bin Shen, Yongjun Zhang, Yashar Komijani, Michael Nicklas, Robert Borth, An Wang, Ye Chen, Zhiyong Nie, Rui Li, Xin Lu, *et al.*, “Strange-metal behaviour in a pure ferromagnetic Kondo lattice,” *Nature* **579**, 51–55 (2020).
- [12] G. R. Stewart, “Non-Fermi-liquid behavior in  $d$ - and  $f$ -electron metals,” *Rev. Mod. Phys.* **73**, 797–855 (2001).
- [13] Q. Y. Chen, X. B. Luo, D. H. Xie, M. L. Li, X. Y. Ji, R. Zhou, Y. B. Huang, W. Zhang, W. Feng, Y. Zhang, L. Huang, Q. Q. Hao, Q. Liu, X. G. Zhu, Y. Liu, P. Zhang, X. C. Lai, Q. Si, and S. Y. Tan, “Orbital-Selective Kondo Entanglement and Antiferromagnetic Order in  $\text{USb}_2$ ,” *Phys. Rev. Lett.* **123**, 106402 (2019).
- [14] Ioannis Giannakis, Justin Leshen, Mariam Kawai, Sheng Ran, Chang-Jong Kang, Shanta R. Saha, Y. Zhao, Z. Xu, J. W. Lynn, Lin Miao, L. Andrew Wray, Gabriel Kotliar, Nicholas P. Butch, and Pegor Aynajian, “Orbital-selective Kondo lattice and enigmatic  $f$  electrons emerging from inside the antiferromagnetic phase of a heavy fermion,” *Sci. Adv.* **5**, eaaw9061 (2019).
- [15] N. B. Perkins, M. D. Núñez Regueiro, B. Coqblin, and J. R. Iglesias, “Underscreened Kondo lattice model applied to heavy fermion uranium compounds,” *Phys. Rev. B* **76**, 125101 (2007).
- [16] Jooseop Lee, Masaaki Matsuda, John A. Mydosh, Igor Zaliznyak, Alexander I. Kolesnikov, Stefan Söllow, Jacob P. C. Ruff, and Garrett E. Granroth, “Dual Nature of Magnetism in a Uranium Heavy-Fermion System,” *Phys. Rev. Lett.* **121**, 057201 (2018).
- [17] Dai Aoki, Andrew Huxley, Eric Ressouche, Daniel Braithwaite, Jacques Flouquet, Jean-Pascal Brison, Elsa Lhotel, and Carley Paulsen, “Coexistence of superconductivity and ferromagnetism in  $\text{URhGe}$ ,” *Nature* **413**, 613–616 (2001).
- [18] Christian Pfeiderer, “Superconducting phases of  $f$ -electron compounds,” *Rev. Mod. Phys.* **81**, 1551–1624 (2009).
- [19] S. Doniach, “The Kondo lattice and weak antiferromagnetism,” *Physica B+C* **91**, 231–234 (1977).
- [20] Yi-feng Yang, Zachary Fisk, Han-Oh Lee, J. D. Thompson, and David Pines, “Scaling the Kondo lattice,” *Nature* **454**, 611–613 (2008).
- [21] S. Kondo, D. C. Johnston, C. A. Swenson, F. Borsa, A. V. Mahajan, L. L. Miller, T. Gu, A. I. Goldman, M. B. Maple, D. A. Gajewski, E. J. Freeman, N. R. Dilley, R. P. Dickey, J. Merrin, K. Kojima, G. M. Luke, Y. J. Uemura, O. Chmaissem, and J. D. Jorgensen, “ $\text{LiV}_2\text{O}_4$ : A Heavy Fermion Transition Metal Oxide,” *Phys. Rev. Lett.* **78**, 3729–3732 (1997).
- [22] C. Urano, M. Nohara, S. Kondo, F. Sakai, H. Takagi, T. Shiraki, and T. Okubo, “ $\text{LiV}_2\text{O}_4$  Spinel as a Heavy-Mass Fermi Liquid: Anomalous Transport and Role of Geometrical Frustration,” *Phys. Rev. Lett.* **85**, 1052–1055 (2000).
- [23] Wataru Kobayashi, Ichiro Terasaki, Jun-ichi Takeya, Ichiro Tsukada, and Yoichi Ando, “A Novel Heavy-Fermion State in  $\text{CaCu}_3\text{Ru}_4\text{O}_{12}$ ,” *J. Phys. Soc. Jpn.* **73**, 2373–2376 (2004).
- [24] J.-G. Cheng, J.-S. Zhou, Y.-F. Yang, H. D. Zhou, K. Matsubayashi, Y. Uwatoko, A. MacDonald, and J. B. Goodenough, “Possible Kondo Physics near a Metal-Insulator Crossover in the  $A$ -Site Ordered Perovskite  $\text{CaCu}_3\text{Ir}_4\text{O}_{12}$ ,” *Phys. Rev. Lett.* **111**, 176403 (2013).
- [25] Y. P. Wu, D. Zhao, A. F. Wang, N. Z. Wang, Z. J. Xiang, X. G. Luo, T. Wu, and X. H. Chen, “Emergent Kondo Lattice Behavior in Iron-Based Superconductors  $\text{AFe}_2\text{As}_2$  ( $A = \text{K}, \text{Rb}, \text{Cs}$ ),” *Phys. Rev. Lett.* **116**, 147001 (2016).
- [26] Igor A. Zaliznyak, Zhijun Xu, John M. Tranquada, Genda Gu, Alexei M. Tsvelik, and Matthew B. Stone, “Unconventional Temperature Enhanced Magnetism in  $\text{Fe}_{1.1}\text{Te}$ ,” *Phys. Rev. Lett.* **107**, 216403 (2011).
- [27] Hisashi Kotegawa, Masaaki Matsuda, Feng Ye, Yuki Tani, Kohei Uda, Yoshiki Kuwata, Hideki Tou, Eiichi Matsuoka, Hitoshi Sugawara, Takahiro Sakurai, Hitoshi Ohta, Hisatomo Harima, Keiki Takeda, Junichi Hayashi, Shingo Araki, and Tatsuo C. Kobayashi, “Helimagnetic Structure and Heavy-Fermion-Like Behavior in the Vicinity of the Quantum Critical Point in  $\text{Mn}_3\text{P}$ ,” *Phys. Rev. Lett.* **124**, 087202 (2020).
- [28] Minsoo Kim, Junyoung Kwon, Choong H. Kim, Younsik Kim, Daun Chung, Hanyoung Ryu, Jongkeun Jung, Beom Seo Kim, Dongjoon Song, Jonathan D. Denlinger, Moonsoo Han, Yoshiyuki Yoshida, Takashi Mizokawa, Wonshik Kyung, and Changyoung Kim, “Signature of Kondo hybridisation with an orbital-selective Mott phase in  $4d \text{Ca}_{2-x}\text{Sr}_x\text{RuO}_4$ ,” *npj Quantum Mater.* **7**, 59 (2022).
- [29] Yun Zhang, Haiyan Lu, Xiegang Zhu, Shiyong Tan, Wei Feng, Qin Liu, Wen Zhang, Qiuyun Chen, Yi Liu, Xuebing Luo, Donghua Xie, Lizhu Luo, Zhengjun Zhang, and Xinchun Lai, “Emergence of Kondo lattice behavior in a van der Waals itinerant ferromagnet,  $\text{Fe}_3\text{GeTe}_2$ ,” *Sci. Adv.* **4**, eaao6791 (2018).
- [30] Mengting Zhao, Bin-Bin Chen, Yilian Xi, Yanyan Zhao, Hang Xu, Hongrun Zhang, Ningyan Cheng, Haifeng Feng, Jincheng Zhuang, Feng Pan, Xun Xu, Weichang Hao, Wei Li, Si Zhou, Shi Xue Dou, and Yi Du, “Kondo Holes in the Two-Dimensional Itinerant Ising Ferromagnet  $\text{Fe}_3\text{GeTe}_2$ ,” *Nano Lett.* **21**, 6117–6123 (2021).
- [31] Song Bao, Wei Wang, Yanyan Shangguan, Zhengwei Cai, Zhao-Yang Dong, Zhentao Huang, Wenda Si, Zhen Ma, Ryoichi Kajimoto, Kazuhiko Ikeuchi, Shin-ichiro Yano, Shun-Li Yu, Xiangang Wan, Jian-Xin Li, and Jinsheng Wen, “Neutron Spectroscopy Evidence on the Dual Nature of Magnetic Excitations in a van der Waals Metallic Ferromagnet  $\text{Fe}_{2.72}\text{GeTe}_2$ ,” *Phys. Rev. X* **12**, 011022 (2022).
- [32] Yujun Deng, Yijun Yu, Yichen Song, Jingzhao Zhang, Nai Zhou Wang, Zeyuan Sun, Yangfan Yi, Yi Zheng Wu, Shiwei Wu, Junyi Zhu, Jing Wang, Xian Hui Chen, and Yuanbo Zhang, “Gate-tunable room-temperature ferromagnetism in two-dimensional  $\text{Fe}_3\text{GeTe}_2$ ,” *Nature* **563**, 94–99 (2018).
- [33] Zaiyao Fei, Bevin Huang, Paul Malinowski, Wenbo

- Wang, Tiancheng Song, Joshua Sanchez, Wang Yao, Di Xiao, Xiaoyang Zhu, Andrew F May, Weida Wu, H. David Cobden, Jiun-Haw Chu, and Xiaodong Xu, “Two-dimensional itinerant ferromagnetism in atomically thin  $\text{Fe}_3\text{GeTe}_2$ ,” *Nat. Mater.* **17**, 778–782 (2018).
- [34] Bo Liu, Shanshan Liu, Long Yang, Zhendong Chen, Enze Zhang, Zihan Li, Jing Wu, Xuezhong Ruan, Faxian Xiu, Wenqing Liu, Liang He, Rong Zhang, and Yongbing Xu, “Light-Tunable Ferromagnetism in Atomically Thin  $\text{Fe}_3\text{GeTe}_2$  Driven by Femtosecond Laser Pulse,” *Phys. Rev. Lett.* **125**, 267205 (2020).
- [35] Guolin Zheng, Wen-Qiang Xie, Sultan Albarakati, Meri Algarni, Cheng Tan, Yihao Wang, Jingyang Peng, James Partridge, Lawrence Farrar, Jiabao Yi, Yimin Xiong, Mingliang Tian, Yu-Jun Zhao, and Lan Wang, “Gate-Tuned Interlayer Coupling in van der Waals Ferromagnet  $\text{Fe}_3\text{GeTe}_2$  Nanoflakes,” *Phys. Rev. Lett.* **125**, 047202 (2020).
- [36] Zhe Wang, Deepak Sapkota, Takashi Taniguchi, Kenji Watanabe, David Mandrus, and Alberto F Morpurgo, “Tunneling spin valves based on  $\text{Fe}_3\text{GeTe}_2/\text{hBN}/\text{Fe}_3\text{GeTe}_2$  van der Waals heterostructures,” *Nano Lett.* **18**, 4303–4308 (2018).
- [37] Xiao Wang, Jian Tang, Xiuxin Xia, Congli He, Junwei Zhang, Yizhou Liu, Caihua Wan, Chi Fang, Chenyang Guo, Wenlong Yang, Yao Guang, Xiaomin Zhang, Hongjun Xu, Jinwu Wei, Mengzhou Liao, Xiaobo Lu, Jiafeng Feng, Xiaoxi Li, Yong Peng, Hongxiang Wei, Rong Yang, Dongxia Shi, Xixiang Zhang, Zheng Han, Zhidong Zhang, Guangyu Zhang, Guoqiang Yu, and Xiufeng Han, “Current-driven magnetization switching in a van der Waals ferromagnet  $\text{Fe}_3\text{GeTe}_2$ ,” *Sci. Adv.* **5**, eaaw8904 (2019).
- [38] Jian-Xin Zhu, Marc Janoschek, D. S. Chaves, J. C. Cezar, Tomasz Durakiewicz, Filip Ronning, Yasmine Sassa, Martin Mansson, B. L. Scott, N. Wakeham, Eric D. Bauer, and J. D. Thompson, “Electronic correlation and magnetism in the ferromagnetic metal  $\text{Fe}_3\text{GeTe}_2$ ,” *Phys. Rev. B* **93**, 144404 (2016).
- [39] M. Corasaniti, R. Yang, K. Sen, K. Willa, M. Merz, A. A. Haghighirad, M. Le Tacon, and L. Degiorgi, “Electronic correlations in the van der Waals ferromagnet  $\text{Fe}_3\text{GeTe}_2$  revealed by its charge dynamics,” *Phys. Rev. B* **102**, 161109 (2020).
- [40] Bin Chen, JinHu Yang, HangDong Wang, Masaki Imai, Hiroto Ohta, Chishiro Michioka, Kazuyoshi Yoshimura, and MingHu Fang, “Magnetic Properties of Layered Itinerant Electron Ferromagnet  $\text{Fe}_3\text{GeTe}_2$ ,” *J. Phys. Soc. Jpn.* **82**, 124711 (2013).
- [41] X. Xu, Y. W. Li, S. R. Duan, S. L. Zhang, Y. J. Chen, L. Kang, A. J. Liang, C. Chen, W. Xia, Y. Xu, P. Malinowski, X. D. Xu, J.-H. Chu, G. Li, Y. F. Guo, Z. K. Liu, L. X. Yang, and Y. L. Chen, “Signature for non-stoner ferromagnetism in the van der waals ferromagnet  $\text{Fe}_3\text{GeTe}_2$ ,” *Phys. Rev. B* **101**, 201104 (2020).
- [42] S. Calder, A. I. Kolesnikov, and A. F. May, “Magnetic excitations in the quasi-two-dimensional ferromagnet  $\text{Fe}_{3-x}\text{GeTe}_2$  measured with inelastic neutron scattering,” *Phys. Rev. B* **99**, 094423 (2019).
- [43] Xiaojian Bai, Frank Lechermann, Yaohua Liu, Yongqiang Cheng, Alexander I. Kolesnikov, Feng Ye, Travis J. Williams, Songxue Chi, Tao Hong, Garrett E. Granroth, Andrew F. May, and Stuart Calder, “Antiferromagnetic fluctuations and orbital-selective Mott transition in the van der Waals ferromagnet  $\text{Fe}_{3-x}\text{GeTe}_2$ ,” *Phys. Rev. B* **106**, L180409 (2022).
- [44] S. P. Bayrakci, T. Keller, K. Habicht, and B. Keimer, “Spin-Wave Lifetimes Throughout the Brillouin Zone,” *Science* **312**, 1926–1929 (2006).
- [45] C.-M. Wu, G. Deng, J.S. Gardner, P. Vorderwisch, W.-H. Li, S. Yano, J.-C. Peng, and E. Imamovic, “SIKA—the multiplexing cold-neutron triple-axis spectrometer at ANSTO,” *J. Inst.* **11**, P10009 (2016).
- [46] S. Yano, G. N. Iles, J.-Ch. Peng, and Ch.-M. Wu, “Current Status of the Taiwanese Cold Triple Axis Spectrometer, SIKA, at ANSTO,” *J. Surf. Investig.* **14**, S207–S212 (2020).
- [47] Jun Zhao, D. T. Adroja, Dao-Xin Yao, R. Bewley, Shiliang Li, X. F. Wang, G. Wu, X. H. Chen, Jiangping Hu, and Pengcheng Dai, “Spin waves and magnetic exchange interactions in  $\text{CaFe}_2\text{As}_2$ ,” *Nat. Phys.* **5**, 555–560 (2009).
- [48] Xiang Chen, Igor Krivenko, Matthew B. Stone, Alexander I. Kolesnikov, Thomas Wolf, Dmitry Reznik, Kevin S. Bedell, Frank Lechermann, and Stephen D. Wilson, “Unconventional Hund metal in a weak itinerant ferromagnet,” *Nat. Commun.* **11**, 3076 (2020).
- [49] O. W. Dietrich, J. Als-Nielsen, and L. Passell, “Neutron scattering from the Heisenberg ferromagnets  $\text{EuO}$  and  $\text{EuS}$ . III. Spin dynamics of  $\text{EuO}$ ,” *Phys. Rev. B* **14**, 4923–4945 (1976).
- [50] B. I. Halperin and P. C. Hohenberg, “Scaling Laws for Dynamic Critical Phenomena,” *Phys. Rev.* **177**, 952–971 (1969).
- [51] Yu Liu, V. N. Ivanovski, and C. Petrovic, “Critical behavior of the van der Waals bonded ferromagnet  $\text{Fe}_{3-x}\text{GeTe}_2$ ,” *Phys. Rev. B* **96**, 144429 (2017).
- [52] J. Qi, T. Durakiewicz, S. A. Trugman, J.-X. Zhu, P. S. Riseborough, R. Baumbach, E. D. Bauer, K. Gofryk, J.-Q. Meng, J. J. Joyce, A. J. Taylor, and R. P. Prasankumar, “Measurement of Two Low-Temperature Energy Gaps in the Electronic Structure of Antiferromagnetic  $\text{USb}_2$  Using Ultrafast Optical Spectroscopy,” *Phys. Rev. Lett.* **111**, 057402 (2013).
- [53] Y. P. Liu, Y. J. Zhang, J. J. Dong, H. Lee, Z. X. Wei, W. L. Zhang, C. Y. Chen, H. Q. Yuan, Yi-feng Yang, and J. Qi, “Hybridization Dynamics in  $\text{CeCoIn}_5$  Revealed by Ultrafast Optical Spectroscopy,” *Phys. Rev. Lett.* **124**, 057404 (2020).
- [54] LuoJun Du, Jian Tang, Yanchong Zhao, Xiaomei Li, Rong Yang, Xuerong Hu, Xueyin Bai, Xiao Wang, Kenji Watanabe, Takashi Taniguchi, Dongxia Shi, Guoqiang Yu, Xuedong Bai, Tawfique Hasan, Guangyu Zhang, and Zhipei Sun, “Lattice Dynamics, Phonon Chirality, and Spin-Phonon Coupling in 2D Itinerant Ferromagnet  $\text{Fe}_3\text{GeTe}_2$ ,” *Adv. Funct. Mater.* **29**, 1904734.
- [55] Ming Tang, Junwei Huang, Feng Qin, Kun Zhai, Toshiya Ideue, Zeya Li, Fanhao Meng, Anmin Nie, Linglu Wu, Xiangyu Bi, Caorong Zhang, Ling Zhou, Peng Chen, Caiyu Qiu, Peizhe Tang, Haijun Zhang, Xiangang Wan, Lin Wang, Zhongyuan Liu, Yongjun Tian, Yoshihiro Iwasa, and Hongtao Yuan, “Continuous manipulation of magnetic anisotropy in a van der Waals ferromagnet via electrical gating,” *Nat. Electron.* **6**, 28–36 (2023).
- [56] Yuan Gao, Junsen Wang, Qiaoyi Li, Qing-Bo Yan, Tao Shi, and Wei Li, “Magnon Damping Minimum and Logarithmic Scaling in a Kondo-Heisenberg Ferromagnet,” in submission.